INL/JOU-23-74609-Revision-1

Forward and Inverse Predictive Transient Models of TREAT Using Surrogate Reactivity Models

June 2024

Mustafa Kamel Mohammad Jaradat, Sebastian Schunert, Mark D DeHart, Frederick N Gleicher, Vincent M Laboure

Changing the World's Energy Future

INL is a U.S. Department of Energy National Laboratory operated by Battelle Energy Alliance, LLC

DISCLAIMER

This information was prepared as an account of work sponsored by an agency of the U.S. Government. Neither the U.S. Government nor any agency thereof, nor any of their employees, makes any warranty, expressed or implied, or assumes any legal liability or responsibility for the accuracy, completeness, or usefulness, of any information, apparatus, product, or process disclosed, or represents that its use would not infringe privately owned rights. References herein to any specific commercial product, process, or service by trade name, trade mark, manufacturer, or otherwise, does not necessarily constitute or imply its endorsement, recommendation, or favoring by the U.S. Government or any agency thereof. The views and opinions of authors expressed herein do not necessarily state or reflect those of the U.S. Government or any agency thereof.

INL/JOU-23-74609-Revision-1

Forward and Inverse Predictive Transient Models of TREAT Using Surrogate Reactivity Models

Mustafa Kamel Mohammad Jaradat, Sebastian Schunert, Mark D DeHart, Frederick N Gleicher, Vincent M Laboure

June 2024

Idaho National Laboratory
Idaho Falls, Idaho 83415

http://www.inl.gov

Prepared for the
U.S. Department of Energy
Under DOE Idaho Operations Office
Contract DE-AC07-05ID14517

Highlights

Forward and Inverse Predictive Transient Models of TREAT Using Surrogate Reactivity Models

Mustafa K. Jaradat, Sebastian Schunert, Frederick N. Gleicher, Vincent M. Labouré, Mark D. DeHart

- Novel transient models were developed to predict the power evolution and control rod axial position during the transient experiments of the TREAT facility.
- The models leverage steady-state Monte Carlo calculations, point kinetics, surrogate reactivity models, and proportional controller.
- Validation results show a good agreement with measured power and control rod axial position during the experiments.

Forward and Inverse Predictive Transient Models of TREAT Using Surrogate Reactivity Models

Mustafa K. Jaradat[a], Sebastian Schunert[a], Frederick N. Gleicher[a], Vincent M. Labouré[a], Mark D. DeHart[a]

[a]*Reactor Physics Methods and Analysis, Idaho National Laboratory, 2525 Fremont Avenue, Idaho Falls, 83415, Idaho, USA*

Abstract

In this work, we present two novel approaches for predicting the power evolution and control rod height of the Transient Reactor Test Facility (TREAT) to support experiment modeling; specifically, transient analysis of the NASA-sponsored Sirius series of experiments. These approaches utilize steady-state Monte Carlo model, point kinetics model, and surrogate models to predict power evolution and control rod axial position during transient experiments Both approaches were tested and validated against several Sirius experiments that were performed in the TREAT facility at different power levels. The validation test results show very good agreement with the experimental data, and the models were able to accurately predict the power evolution and the axial control rod position with an average error within 3.0%. This indicates that these approaches will help the reactor engineering team of the TREAT facility in preparing and predicting the power and temperature of the experiment.

Keywords: Transient, Point Kinetics, Reactivity, Surrogate Model, TREAT, Sirius Experiments

1. Introduction

Solving multiphysics time-dependent problems accurately and efficiently is challenging. In the field of nuclear reactor physics, several improvements were made toward enhancing the efficiency and accuracy of numerical methods specifically for steady-state solutions of the neutron transport equation. One example is the Monte Carlo method. However, several methods were developed for solving time-dependent or spatial kinetics problems with approximations applied to certain problems. The Monte Carlo method is widely used for steady state calculations as it provides high-fidelity solutions but for spatial kinetics and large problems the computational expense is still burdensome, and current time-dependent Monte Carlo methods are limited to very short transients [1, 2, 3]. In deterministic spatial kinetics methods, the biggest challenge is preparing and interpolating accurate kinetics parameters [4] cross-section data files that cover the entire range of the problem for any anticipated scenario. Also, deterministic methods employ the multigroup approximation to the neutron transport equation, and selecting the energy group structure varies with reactor types, and it might not be valid for spatial kinetics problems with tremendous spectral changes.

The high computational cost of the Monte Carlo methods can be overcome by coupling high-fidelity methods (Monte Carlo) to low-fidelity methods (e.g., point kinetics). As an example of obtaining the time-dependent solution of the neutron flux, the high-fidelity solution will provide the changes in the neutron flux shape utilizing a steady-state Monte Carlo solution, while the low-fidelity solution updates the amplitude of the neutron flux using the point kinetics approximation and preserving the reactor integral quantities. However, the above approach requires performing steady-state Monte Carlo calculations at every change in the system's main parameters, such as moving control rods and/or change in temperature, which might be infeasible for large reactor problems. In this work, we developed an accurate and efficient approach leveraging the high-fidelity Monte Carlo steady-state solution, point kinetics approximation, and machine learning capabilities to perform time-dependent calculations. We applied the developed model to the Transient Reactor Test Facility (TREAT) for validation purposes and to support the National Aeronautics and Space Administration (NASA) experiment design and irradiation of nuclear fuel for space application by providing the necessary data prior to the experiment.

NASA is considering using nuclear thermal propulsion (NTP) in their rocket design to replace chemical rockets [5]. NASA is collaborating with Idaho National Laboratory (INL) to design and test such nuclear materials for space application at the TREAT facility under prototypical conditions of increasing the fuel temperature

to a very high level from cold conditions in a short period. This is accompanied with intense radiation fields due to rapid change of the sample and reactor power that can be achieved in the TREAT facility [6, 7]. A series of experiments are being designed and performed at the TREAT facility for testing NASA's NTP fuel materials known as Sirius. The main objective of the Sirius experiments is to examine the performance of NTP fuel materials when it is subjected to high-temperature ramps and high-power rates to mimic high irradiation fields that are representative of NTP systems [8].

Modeling and simulation is used prior to TREAT experiments to evaluate the response of the reactor and specimen to different sequences of control rod motion. The results of these simulations are used to tweak the prescribed control rod motion to achieve the desired experiment conditions during the transient. Among the codes used for this purpose is the Multiphysics Object Oriented Simulation Environment (MOOSE) [9]. Recent pre-transient analysis includes thermal analysis of the Sirius experiments [10] with the fuel performance code BISON [11], neutronics evaluation of the transient tests using the neutronics analysis tool Griffin [12], and the stochastic tools module of the MOOSE framework [13]. The ultimate goal of the analysis performed is to develop a multiphysics model that will be able to predict control rod movements to achieve desired time-dependent conditions in the experimental setup. To this end, the multiphysics model needs to be able to predict reactor power from control rod motion, specimen power from reactor power, and experiment temperature and stresses from experiment power.

In this work, we present two different types of predictive transient models and their application to Sirius experiments performed at the TREAT facility, namely the *forward* and *inverse* models. The forward model provides a prediction of the power level given the control rod motion, while the inverse model computes control rod movement given a power. We validate both models with experimental data from the Sirius experiments. This work focuses entirely on the core conditions and does not elaborate on how to obtain the power deposited in the experiment and its resulting temperature evolution. A follow-up study will be published focusing on these aspects for the Sirius-2c experiment. In previous work, we presented fully coupled calculations to predict Sirius-3 specimen temperature [10] and reactor power prediction using the measured axial position of the control rod for Sirius-1 experiments. The main focus of this work is to provide details of the developed predictive transient models and their application to the TREAT facility for power and control rod position prediction.

This paper is organized as follows: Sect. 2 discusses the theory and methodologies utilized in this work, along with governing equations. Sect. 3 provides a brief description of the TREAT facility and the developed Monte Carlo model, along with

the control rod worth validation tests and a reactor parametric study on the reactivity worth change of the control rods. Sect. 4 discusses the predictive transient models developed to predict the reactor total power and axial position and movements of the control rods, and the data generation procedure for calculating the reactivity and control rod worth. Sect. 5 presents validation test results of the predictive transient models for Sirius-1, Sirius-2c, and Sirius-3 experiments at different power levels. Finally, Sect. 6 provides a summary, future work, and improvements of the developed predictive transient models and their deployment to support future reactor and experiment designs.

2. Theory and Methodology

The solution of the time-dependent neutron transport equation can be achieved in several ways considering high-order deterministic and stochastic approaches to resolve the details of the flux including both shape and amplitude. The vast majority of deterministic neutronics methods use the multigroup approximation to discretize the energy variable. Time is discretized using a finite difference approach to recast the transient equations as a fixed source problem. The most challenging part of this approach is preparing and tabulating the multigroup cross sections accurately based on the system parameters and its accuracy depends on the number of points considered in generating these data sets. Also, selecting the time step size requires some advanced knowledge of the simulated transient [14]. Oftentimes, an improved quasi-static method is used to accelerate the solution process and obtain a more accurate solution for a given run time [3, 15].

On the other hand, the time-dependent Monte Carlo method is computationally very expensive (considering very long transients), and it is very challenging to perform multiphysics-coupled calculations, which require cross sections updates based on temperature and density spatial distributions. However, a high-order/low-order (HOLO) method can be employed to solve time-dependent problems efficiently. In this approach, the high-order method is used to update the neutron flux shape, while the low-order method advances the problem in time by updating the amplitude [15].

In this work, we employ the HOLO method to solve spatial kinetics problems utilizing the steady-state Monte Carlo method to obtain high-fidelity solutions and update the neutron flux shape, while the point kinetics equation (PKE) is used as a lower-fidelity solution to update the amplitude of the neutron flux. However, we employ an offline approach to update the Monte Carlo solution at each time point by incorporating machine learning capabilities to update the shape instead of performing a costly Monte Carlo solve during the simulation. First, we discuss the HOLO method that is being used to solve spatial kinetics problem and, in the next sections, the offline approach will be discussed in detail. To describe the approach that is being utilized in this work, we consider the time-dependent neutron transport equation in diffusion form for simplicity as shown in Eq. (1) and Eq. (2) for simplicity.

$$\frac{1}{v(E)}\frac{\partial\phi(\vec{r},E,t)}{\partial t} - \nabla\cdot D(\vec{r},E,t)\nabla\phi(\vec{r},E,t) + \Sigma_t(\vec{r},E,t)\phi(\vec{r},E,t) =$$
$$\int_0^\infty dE'\Sigma_s(E'\to E)\phi(E') + \frac{(1-\beta)\chi_p(\vec{r},E,t)}{k_{eff,ss}}\int_0^\infty dE'\nu\Sigma_f(\vec{r},E',t)\phi(\vec{r},E',t) \quad (1)$$
$$+\sum_{k=1}^{K}\chi_{dk}(\vec{r},E,t)\lambda_k C_k(\vec{r},t),$$

$$\frac{\partial C_k(\vec{r},t)}{\partial t} + \lambda_k C_k(\vec{r},t) = \frac{\beta_k}{k_{eff,ss}}\int_0^\infty dE'\nu\Sigma_f(\vec{r},E',t)\phi(\vec{r},E',t), \qquad k=1,2,.....,K, \quad (2)$$

where:

t = Time variable.

E = Neutron energy.

$\vec{r}$ = Position vector.

v = Neutron speed.

ϕ = Neutron scalar flux.

D = Neutron diffusion coefficient.

Σ_x = Neutron cross section of type x. t: total; f: fission; s: scattering.

ν = Number of neutrons emitted per fission.

χ_p = Fraction of prompt neutrons emitted at energy E.

k =Delayed neutron precursor family index.

C_k = Concentration of delayed neutron precursor of family k.

χ_{dk} = =Fraction of delayed neutrons emitted at energy E from precursor family k.

β_k =Delayed neutron fraction of family k.

λ_k =Decay constant of precursor family k.

β =Delayed neutron fraction.

$k_{eff,ss}$ = Effective multiplication factor or eigenvalue of the problem at initial steady-state conditions prior to the start of the transient

The neutron flux ($\phi(\vec{r},E,t)$) can be decomposed into a shape and amplitude components assuming the flux shape ($\Phi(\vec{r},E,t)$) is slowly varying in time while the amplitude ($p(t)$) is rapidly changing as

$$\phi(\vec{r},E,t) = p(t)\Phi(\vec{r},E,t). \quad (3)$$

To make this decomposition unique, the time variation of the shape functions is constrained as

$$\int_0^\infty dE \int_V d\vec{r}\phi_0^*(\vec{r},E)v^{-1}(E)\phi(\vec{r},E,t) = \int_0^\infty dE \int_V d\vec{r}\phi_0^*(\vec{r},E)v^{-1}(E)\phi_0(\vec{r},E) = K_0, \tag{4}$$

where K_0 is a constant, $\phi_0^*(\vec{r},E)$ is a weighting function (e.g., the adjoint steady-state solution), and $\phi_0(\vec{r},E)$ is the steady-state neutron flux solution. Multiplying Eq. (1) and Eq. (2) by the weighting function and integrating over space and energy we can derive the exact point kinetic equations as

$$\frac{dp}{dt} = \frac{\rho(t)-\beta_{\text{eff}}(t)}{\Lambda(t)}p(t) + \sum_{k=1}^{K}\lambda_k c_k(t), \tag{5}$$

$$\frac{dc_k}{dt} = \frac{\beta_k(t)}{\Lambda(t)}p(t) - \lambda_k c_k(t), \quad k = 1,2,.....,K, \tag{6}$$

where c_k, β_k, and λ_k are the modified delayed neutron precursor concentration, delayed neutron fraction, and decay constant of the delayed neutron group k, respectively. ρ is the total reactivity of the system, β_{eff} is the effective delayed neutron fraction, and Λ is the neutron mean generation time. The full derivation of the point kinetic equations is discussed in detail in Reference [16].

The solution of Eq. (5) and Eq. (6) is straightforward, and usually a very small time step size is utilized. Thus, the neutron flux amplitude is updated at each time step. However, the solution of the neutron flux shape is updated at coarser time scale to reduce computational time and produce an efficient solution, which can be obtained from solving the steady-state neutron transport equation assuming the transient is slow enough and can be approximated by instantaneous eigenstates [15]. Ignoring the time dependency in Eq. (1) and Eq. (2) and combining the prompt and delayed fission sources into a total fission source, then the steady-state neutron transport equation can be derived as

$$\begin{aligned} -\nabla\cdot D^n(\vec{r},t)\nabla\phi^n(\vec{r},E) + \Sigma_t^n(\vec{r},E)\phi^n(\vec{r},E) = &\int_0^\infty dE'\Sigma_s^n(E'\to E)\phi^n(E') \\ &+\frac{\chi_p(\vec{r},E)}{k_{\text{eff}}^n}\int_0^\infty dE'\Sigma_f^n(\vec{r},E')\phi^n(\vec{r},E'), \end{aligned} \tag{7}$$

where n denotes time step number and k_{eff}^n is the eigenvalue or effective multiplication factor at time point n. Simultaneously solving the point kinetics equations (ampli-

tude update) and the steady state transport equation (shape update) constitute the HOLO approach to obtain an approximated time-dependent solution. The main concern is how often the shape solution will be updated so that the kinetics parameters can be accurate. The measured values of the kinetics parameters can be utilized in the calculation if available or they can be obtained from Monte Carlo steady-state calculations, while the total or net reactivity introduced into the system is typically calculated at each time step assuming the inserted reactivity ρ_{CR} (i.e., due to control rod movement) and the feedback reactivity ρ_{FB} (i.e., due to temperature changes) as

$$\rho(t) = \rho_{CR}(t) + \rho_{FB}(t). \tag{8}$$

In most cases, the system parameters are tightly related, and any change in any of one them will have an impact on the others. As an example, the TREAT facility control rod worth and temperature feedback coefficient are highly interrelated and change depending on the state of the system. Thus, using a fixed control rod worth and a constant feedback coefficient, as in typical point kinetics approaches, will lead to miscalculating the total reactivity of the system. Instead, the total reactivity can be estimated from the change in the eigenvalue of the system at two different states of the system as

$$\rho(t) = \frac{1}{k_{eff,ss}} - \frac{1}{k_{\text{eff}}(t)}, \tag{9}$$

where $k_{eff,ss}$ is the eigenvalue of the system at initial steady-state conditions prior to the start of the transient, while $k_{\text{eff}}(t)$ is the eigenvalue of the system at time t adopting the latest changes in the system. In order to fulfill the above relation, online steady-state calculations need to be performed at each time step, which will be very cumbersome and expensive computationally, especially for a problem of large size and considering a small time step size.

We introduce a new approach to eliminate the need for performing online steady-state eigenvalue calculations to obtain $k_{\text{eff}}(t)$ at each time step by tabulating the k_{eff} as a function of system parameters and leveraging machine learning capabilities, specifically polynomial regression, to predict the system reactivity offline using pre-calculated data sets that cover a wide range of system changes. In this way, the reactivity of the system can be calculated knowing altered parameters and utilizing a surrogate model at each time step without the need for performing eigenvalue calculations.

3. TREAT Facility

TREAT is a thermal test facility designed and constructed at INL in the 1950s. It was specifically designed to test materials under transient conditions ranging from mild to severe accident conditions [17]. After being shut down for 24 years, the operation of TREAT was resumed in 2018 to conduct more experiments [18]. This section provides an overview of the TREAT facility, a description of the TREAT Monte Carlo model, a control rod worth validation tests, and a reactor parametric study.

3.1. Overview of The Facility

The TREAT core consists of a 19 by 19 square lattice with a fuel element pitch of 10.16 cm. The fuel is made of highly enriched uranium (HEU) elements dispersed in a graphite matrix. The fuel element has an octagonal shape near the element corners to form air-cooling flow channels between elements with an element axial length of approximately 255 cm. The graphite acts as a heat sink, and it resulted in having a strong negative temperature feedback since the fuel and moderator are forming a homogeneous mixture. Radially, the reactor core is surrounded by about 61 cm thick graphite reflector and concrete shielding. The reactor is air-cooled and mainly used for post-transient heat removal. Also, the TREAT facility features a large inherent negative temperature feedback, a central experiment irradiation position, and several rapid control and shutdown mechanisms [19]. Detailed description of the reactor can be found in reference [20]. Figure 1 shows a radial view of the TREAT facility [21].

The TREAT facility is equipped with three reactivity control mechanisms made of boron carbide, namely compensation control (C/C), control shutdown (C/S), and transient control rods (C/T). The radial location of each control rod set is shown in Figure 1. Each set is composed of four-rod drives, and each rod drive incorporates two control rods. The C/C rods are very close to the experiment location, but they are at a fully withdrawn position during the transient experiment and are used to shut down the reactor safely post-experiment. The C/T rods are partially inserted into the active core region, and they are withdrawn continuously during the transient so that they will yield the desired reactivity insertion over the course of the transient. The C/S rods are partially inserted into the active core region to make the reactor critical prior to the transient and to compensate for the initial withdrawal of the C/T rods. They remain at a fixed position during the transient [21].

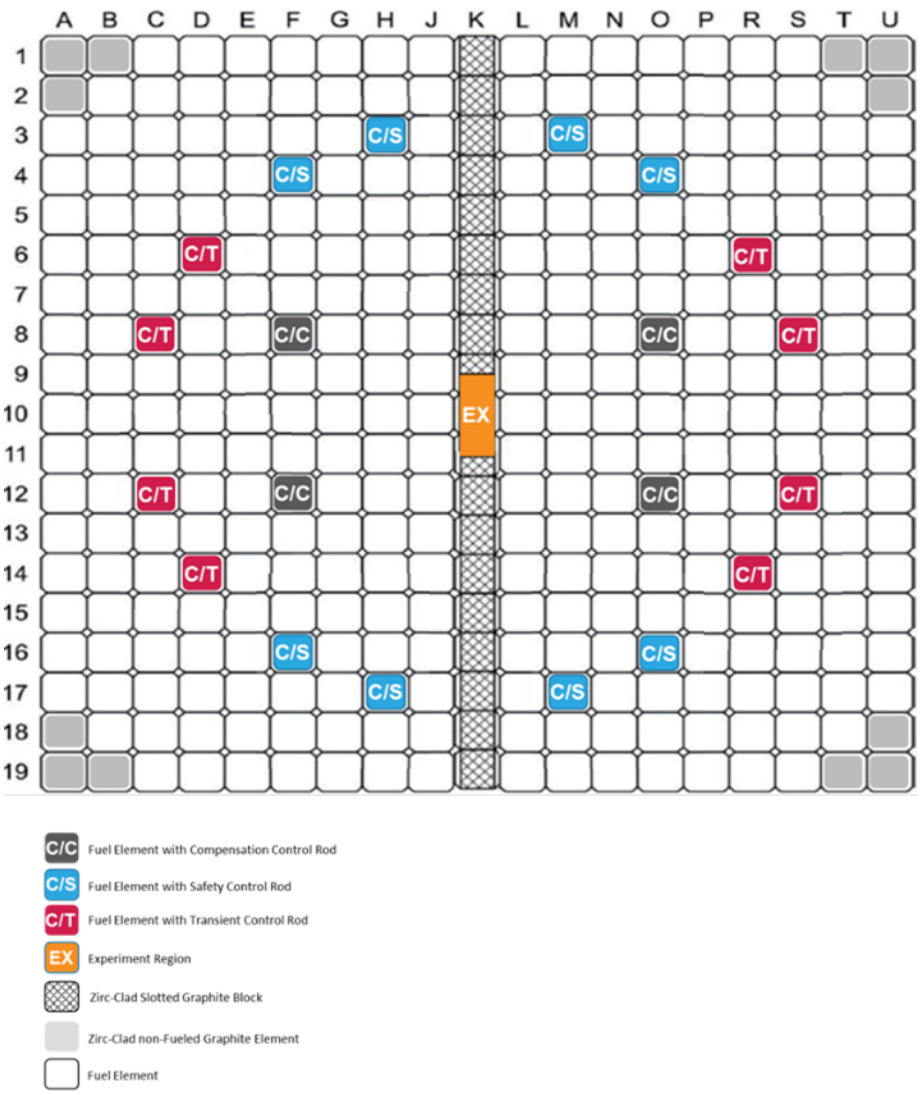

Figure 1: Radial configuration of the TREAT full-slotted core.

3.2. TREAT Monte Carlo Model Validation

The TREAT full-core Serpent [22] model used in this work was developed initially in 2015 for minimum critical core analysis [23] of TREAT and followed by several improvements as discussed in [24, 25, 26]. The model is based on the data and specifications obtained from the BATMAN report [21].

In this work, the Serpent model of TREAT is validated against experimental data of the measured reactivity worth of the C/S control rods. The measurement of the control rod worth was performed with the control rod swap method: the reactor is made critical with one control rod fully inserted and a second rod fully withdrawn, while the remaining control rod positions are adjusted to make the reactor critical at the beginning of the experiment. During the experiment, the fully inserted rod is gradually withdrawn, and the resulting positive reactivity is compensated by inserting the fully withdrawn rod to return to a critical state. The reactivity is measured using both the reactor stable period technique and using the inverse kinetics technique via a reactivity meter that converts the measured neutron signal directly into reactivity. The calculated reactivities are compared with the measured values at each movement of the C/S-4 rod, as shown in Figure 2, and the integral rod worth comparison is shown in Figure 3. The integral rod worth curve was calculated form the differential rod worth curve and by integrating over the axial position. The calculated results show a good agreement with measurement, and most of the points are within statistical uncertainty of the calculations. The measurement uncertainty was not provided by the experimenters. The calculated integral rod worth is within 4.2% of the measured value which is comparable given various uncertainties in experimental and computational measurements.

3.3. Reactor Parametric Study

In the previous subsection, the integral worth of the C/S-4 rod was presented for a single state point, where the other control rods are fixed at a certain height, and the reactor was at zero power, thus, no temperature feedback was involved. In the TREAT facility, there are three sets of control rods, and the axial position of these control rods results in a particular distribution of the neutron flux within the core, which alters the leakage fraction as well. Also, increasing the fuel temperature will significantly impact the control rod reactivity worth due to large negative feedback. The total reactivity of TREAT depends on the axial positions of two control rods and the core average temperature, and this dependence on these parameters are non-separable or correlated.

In order to demonstrate the significance of temperature, control rod positions,

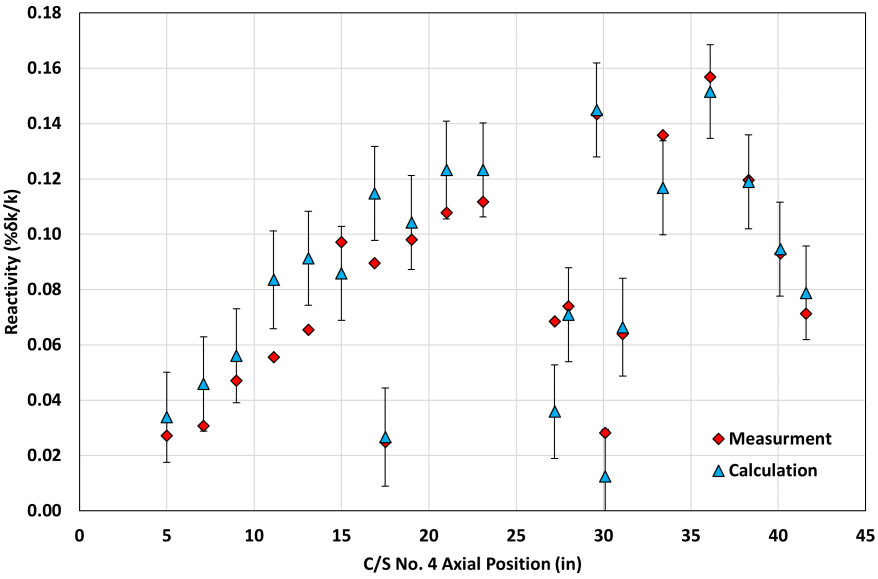

Figure 2: Comparison of measured and calculated reactivities at different axial positions of the C/S-4 control rod.

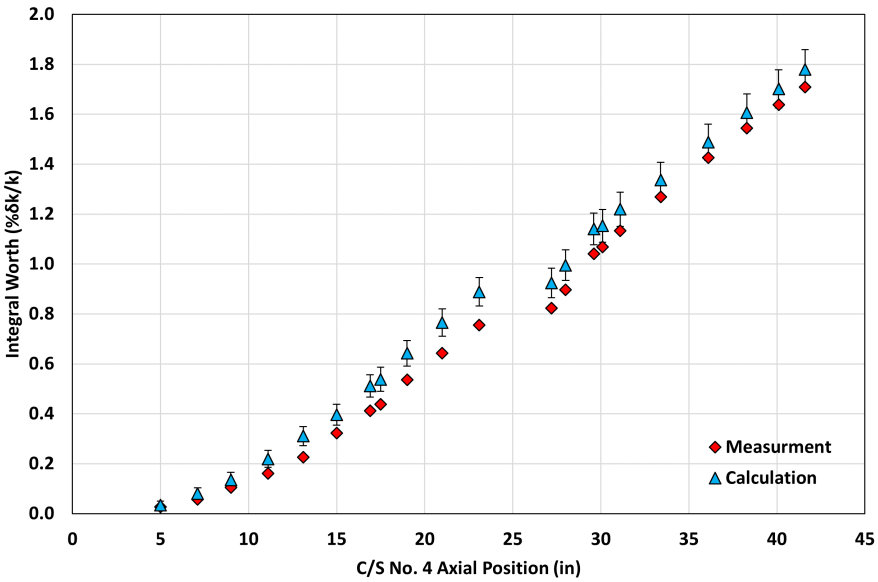

Figure 3: Comparison of measured and calculated integral worth of the C/S-4 control rod.

and their effect on the reactivity worth of a desired control rod, the integral worth of the C/T rods was calculated considering different fuel average temperatures ranging between 294.0 and 700.0 K, and several C/S rods axial positions ranging between 20.0 and 58.0". The integral rod worth map of the C/T rods is presented in Figure 4. The control rod worth changes significantly (11-16 $\%\delta k/k$) and it is enhanced at higher temperatures and increased penetration of the other control rods into the core.

Furthermore, the fuel temperature feedback coefficient was calculated considering several C/S rod axial positions ranging between 20.0 and 58.0" and C/T rod axial positions ranging between 0.0 and 40.0". The temperature feedback coefficient map is provided in Figure 5. The temperature feedback coefficient become less negative at higher temperatures and increased axial control rod positions with a value ranging between -28.0 pcm/K and -18.0 pcm/K.

These results indicate that the control rod worth and fuel temperature feedback coefficient are highly interrelated. However, to explain this significant change in these two parameters, further analysis was performed to demonstrate the changes in the neutron spectrum and core leakage at different states of the core. Figure 6 shows the neutron energy spectrum at different fuel temperatures and C/T axial positions. Increasing the fuel temperature results in hardening the neutron spectrum, specifically it increases the chance of non-fission absorption reaction rate and increases the neutron leakage as well. On the other hand, the insertion of the control rods into the core will enhance the leakage rate as well as the non-fission absorption reaction for a given power. These effects result in a large shift in the neutron spectrum.

The changes in the neutron spectrum at different combinations of fuel temperatures and C/T axial positions are presented in Figure 6. It can be clearly seen that a reduction in the thermal peak and increasing the fast neutron peak at higher temperatures with more insertion of the control rods. Also, Figure 7 provides the leakage fraction map of the neutrons from the core region, which clearly shows higher leakage fractions at higher temperatures. Also, the leakage fraction peaks at 15.0" of the C/T rod height due to neutron flux redistribution, especially the peak region to the bottom of the active core.

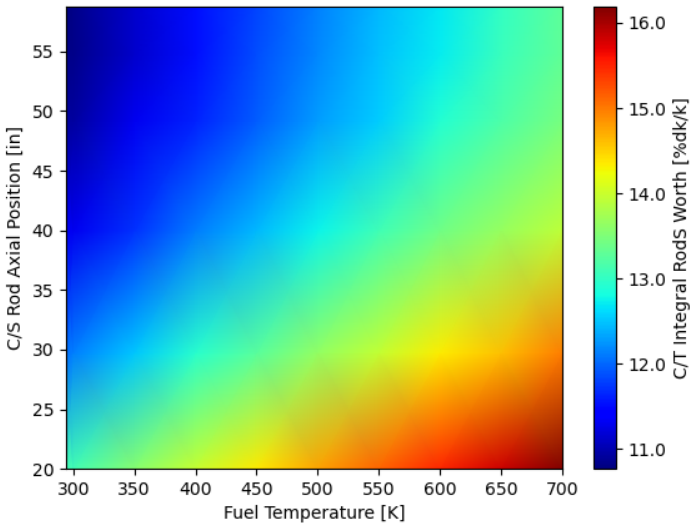

Figure 4: Change of C/T rods integral worth as function of fuel temperature and C/S rod axial position.

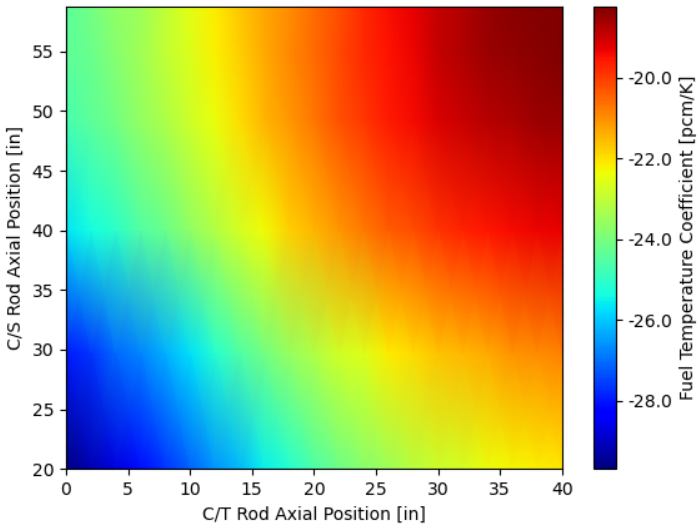

Figure 5: Change of fuel temperature feedback coefficient as function of C/T and C/S rod axial positions.

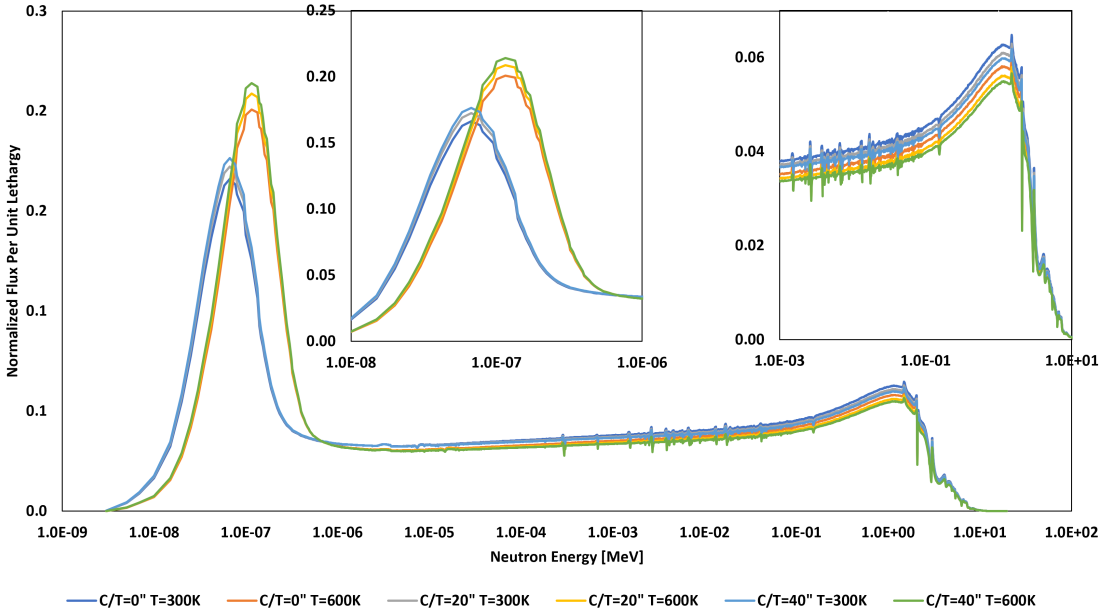

Figure 6: Change of neutron spectrum at different fuel temperature and C/T rod axial position.

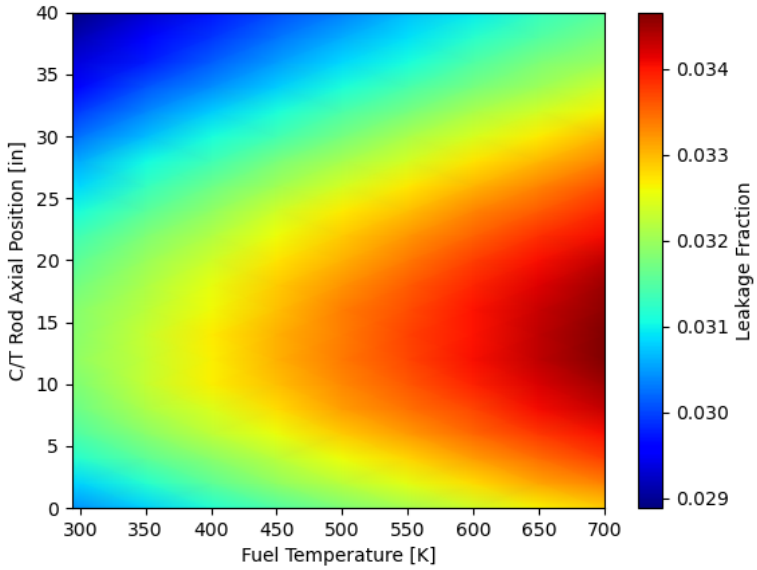

Figure 7: Change of core leakage fraction as function of fuel temperature and C/T rod axial position.

4. Predictive Transient Models

The novel algorithms developed in this work contribute to the ability to design TREAT experiments to meet requirements such as the temperature that needs to be attained in an experiment specimen. TREAT is mostly utilized for material testing under mild to severe irradiation conditions that incorporate high temperatures. To achieve such conditions, the reactor power must be driven to a certain level by adjusting the control rods axial position to introduce the sufficient reactivity into the system. For this reason, the control rods axial movement needs to be determined in advance to achieve the desired test outcomes.

Two transient models were developed to predict the reactor's total power and the axial control rod position during the transient experiments. The first model solves a *forward* problem to predict the reactor power evolution given the control rod motion to calculate the total reactivity introduced in the system. The second model solves an *inverse* problem to predict the axial control rod position given the reactor power. Both models leverage the point kinetics model developed with the reactor multi-physics code Griffin and the steady-state Monte Carlo model developed with the Serpent code of the TREAT facility. This is accomplished by using a surrogate model to predict the inserted reactivity that initiates the transient and a proportional controller that sets the control rod position at every time step and is driven by the difference between computed reactor power and reactor power demand. This section presents the surrogate model (that is used to predict reactivity during the transient), data generation and tabulation procedure. This is followed by a description of the algorithms of predictive transient models of the power and axial control rod positions.

4.1. Surrogate Reactivity Model

The TREAT facility is operated at low power before the start of the transient experiment to establish steady-state conditions. After that, the power starts ramping up as the reactivity is introduced to the system. The main reactivity insertion mechanisms of the TREAT facility are control rod motion and fuel temperature reactivity feedback. In order to determine the total reactivity of the system, the axial positions of all control rods and the fuel temperature must be known. In the previous section, we showed that the impact of both temperature and control rod axial positions on reactivity worth of a desired control rod was significant. During the TREAT transient experiments, only the C/T rod height is adjusted to insert a desired reactivity while other control rods are at fixed positions. However, the C/S rods are partially inserted, and their insertion depth into the core impacts both the C/T rod worth

and the temperature feedback coefficient. We couple the point kinetics solution (low level) to the Serpent Monte Carlo solution (high level). The Serpent steady-state calculations need to be applied at each step if the C/T rods position, C/S rods position, and/or the fuel temperature changed to determine the total reactivity of the system precisely as described by Eq. (9).

To be able to calculate the reactivity during the transient without performing steady state eigenvalue calculations at each time step, a novel approach was introduced to reduce computational time and avoid replicating the same calculations for different transients. It utilizes a surrogate model relying on a set of pre-calculated eigenvalues to predict the total reactivity of the system.

An eigenvalue data set was generated with the TREAT Serpent model considering average fuel temperature, C/S rods axial position, and C/T rods axial position. A total of 1260 data points for reactivity calculations were generated at ten fuel average temperatures 294.0, 300.0, 350.0, 400.0, 450.0, 500.0, 550.0, 600.0, 650.0, and 700.0 K, six C/S rods axial positions at 20.0, 29.7, 40.0, 49.2, 54.8 and 58.8", and 21 C/T rods axial positions ranging between 0.0 and 40.0" with 2.0" intervals. Figure 8 shows all the calculated eigenvalues at each of the C/S and C/T rod's axial positions and fuel average temperature. Each data point was obtained via a Serpent calculation performed with 600 cycles of 10^5 particles after 100 inactive cycles which resulted in eigenvalue uncertainty of 10 pcm. The runtime of each data point is approximately 50 minutes with 480 CPU cores on the INL Sawtooth cluster (Intel Xeon Platinum 8268).

A surrogate model was developed using the stochastic tools module [13] of the MOOSE framework with a polynomial regression surrogate. The generated data with Serpent was used to train the regression surrogate model and generate the coefficients of the polynomial terms. Then this model was used to predict the reactivity knowing the fuel's average temperature, C/S rods axial position, and C/T rod's axial positions. As a verification test, the training data set was fed back to the model to test if the model can reproduce the original data set. This is shown in Figure 9. For comparison purposes, two regression surrogate models were considered: linear and 4^{th} order polynomial. The polynomial regression surrogate model was able to reproduce the original set of data with a maximum error of 20 pcm, while the linear regression surrogate model was mispredicting the reactivity value for most of the points with a maximum error of 2000 pcm.

Also, the linear and polynomial regression surrogate models were tested using a measured control rod axial position during a transient experiment to predict the eigenvalue of the system and compared to the experimental value, which was deduced from the power signal as shown in Figure 10. It can be seen that the polynomial

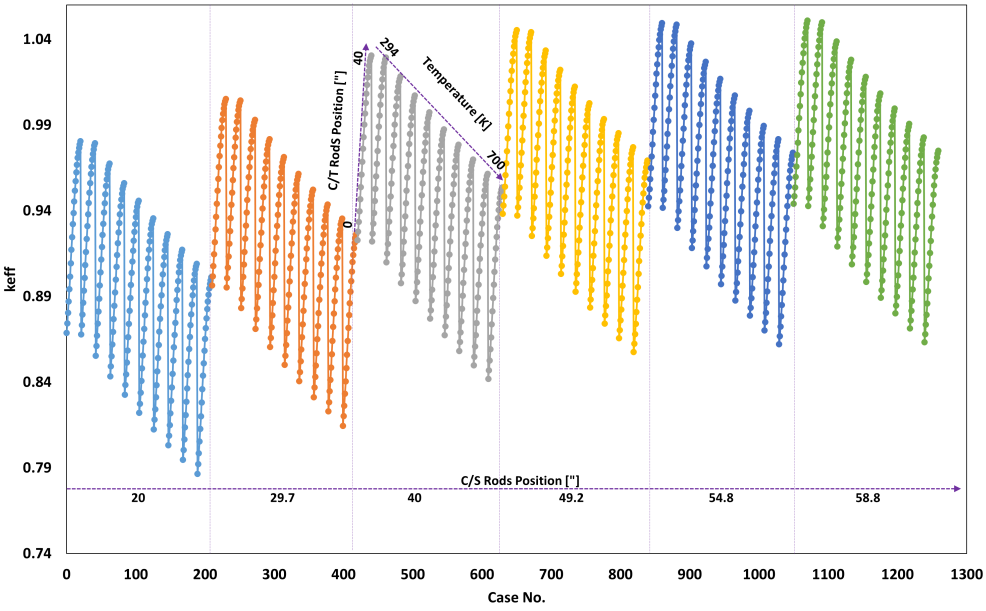

Figure 8: Tabulated eigenvalue as function of the fuel average temperature, C/S and C/T rods axial positions.

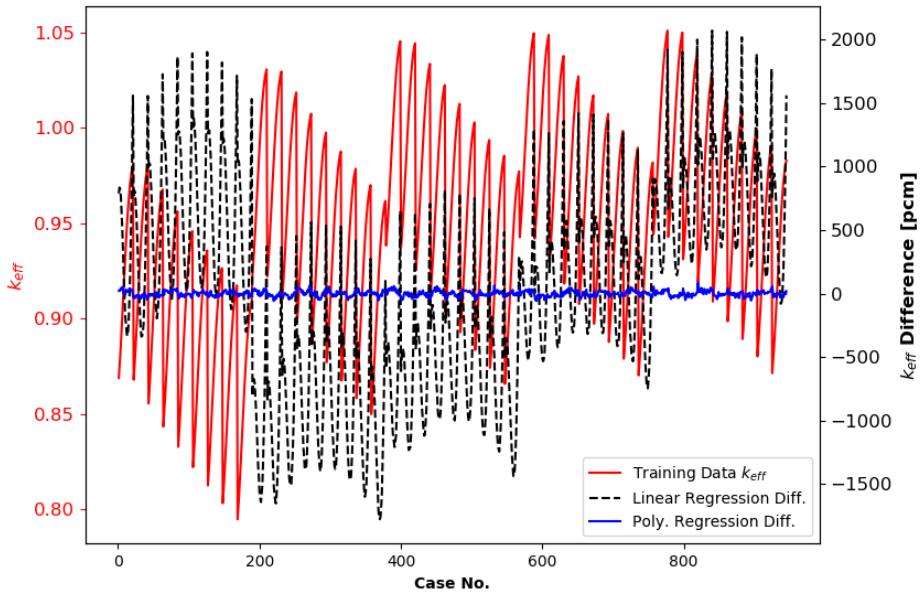

Figure 9: Comparison of the predicted reactivity with surrogate models and original training data set.

regression surrogate model was able to predict the reactivity accurately for the real transient with almost the same error of 10 pcm. On the contrary, a large deviation was observed using the linear regression surrogate model with a significant error variation during the transient. In the remaining analysis, only the polynomial regression surrogate model was used in the predictive transient models.

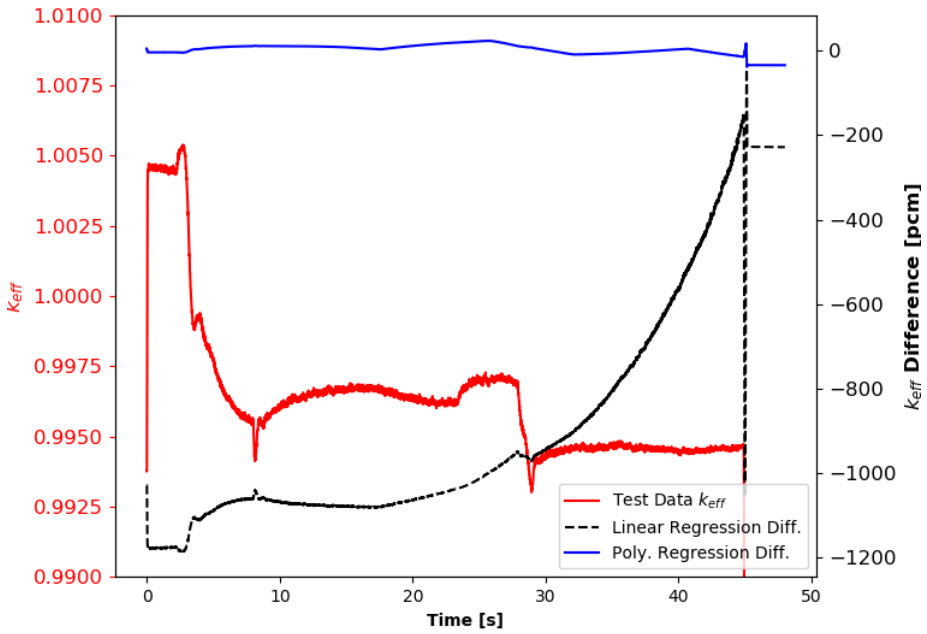

Figure 10: Comparison of the predicted reactivity with surrogate models during transient test.

4.2. Power Prediction Algorithm

The time-dependent total power of the reactor can be obtained by the *forward* solution of the point kinetics equations knowing the time-dependent total reactivity introduced in the system. As discussed in the previous sections, the reactivity can be calculated by knowing the change in the axial position of the control rods and the core average temperature of the TREAT facility.

A predictive transient model of the TREAT facility was developed based on the coupling of high-order Monte Carlo eigenvalue calculations (Serpent steady-state) and low-order point kinetics equations (Eq. (5, 6)) solutions to perform the transient calculation. However, the thermal feedback effect must be considered to perform multiphysics coupled calculations which require temperature calculations.

The temperature distribution of TREAT can be accurately modeled by an adiabatic temperature model (i.e., a model that neglects heat conduction and heat transfer to the ambient air). TREAT transients occur on the timescale of tens of seconds, while heat conduction and heat transfer to the ambient air happen on timescales that are many times longer. Therefore, heat conduction and heat transfer to the air can be neglected during the transient and the temperature in the core is well approximated by an adiabatic temperature model [27].

The forward model couples three physics models to obtain the reactor's total power during the transient experiments along with the fuel average temperature as listed below:

- A point kinetics model that calculates total power and the delayed neutron precursor concentrations given the introduced reactivity in the system at each time point.
- An adiabatic thermal feedback model that calculates the reactor's average temperature given the heat deposited in the system at each time point.
- A surrogate model that performs polynomial regression of precalculated steady-state eigenvalue data set from the Serpent code to predict the reactivity introduced into the system given the core average temperature and axial position of the control rods.

The model is fed with time-dependent control rod positions which are assumed before conducting the experiment or measured during the experiment. A schematic diagram of the calculation workflow and exchanged parameters of the coupled models are shown in Figure 11 [28].

In order to solve the point kinetics equations, the kinetics parameters of the TREAT facility, namely the mean neutron generation time (Λ), the delayed neutron fractions (β), and the decay constants (λ) of each the delayed neutron group must be provided. The current model uses the measured kinetic parameters, as provided in Table 1 [29], to be consistent with the kinetics parameters used in the power measurements. However, using the calculated kinetics parameters by Serpent doesn't have a significant impact on the results except for regions with minimal thermal feedback effects.

4.3. Control Rod Axial Position Prediction Algorithm

The power predictive transient model relies on the measured control rod positions and calculated core average temperature to estimate the total reactivity of the system

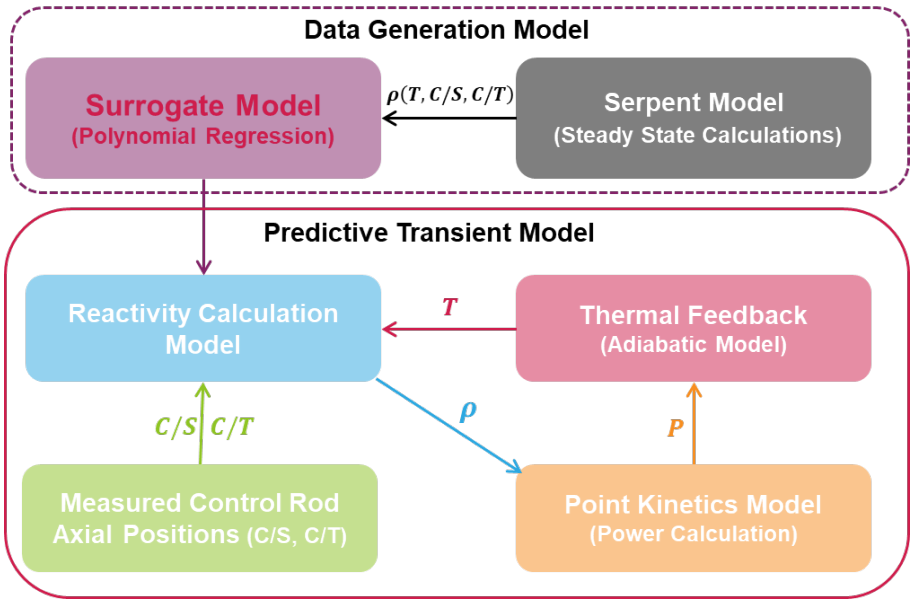

Figure 11: Power predictive transient model calculation workflow.

and perform *forward* power calculations during the transient. Further improvements were made to the power predictive model, and a model was developed with the ability to solve an *inverse* problem to predict control rod positions given a demand power signal during the transient.

The new model solves an *inverse* kinetics equations to determine the demanded reactivity signal (ρ_d) given the demanded power signal (p_d) [30]:

$$\rho_d(t) = \beta_{eff} + \frac{\Lambda}{p_d(t)} \left(\frac{dp_d}{dt} - \sum_{k=1}^{K} \lambda_k c_k(t) \right). \tag{10}$$

Knowing the reactivity that should be inserted into the system, a proportional controller was used to determine the change in the control rod position that satisfies the reactivity demand [14, 31]:

$$H_T(t) = H_{T,0} + k_p(t)\epsilon(t), \tag{11}$$

where $H_T(t)$ is control rod position at time t, $H_{T,0}$ is the previous control rod axial position prior to moving the rod, k_p is proportional coefficient, and ϵ is the error in the reactivity signal computed from the difference of the demanded and predicted reactivities as $\epsilon(t) = \rho_d(t) - \rho(t)$. In the current model, the proportional coefficient

Table 1: Kinetics parameters of the TREAT facility [29].

Group [k]	$\lambda_k[s^{-1}]$	β_k [pcm]
1	0.0124	24.4
2	0.0305	156.7
3	0.111	141.1
4	0.301	282.8
5	1.130	82.6
6	3.000	30.2
Total	-	717.8
Mean Generation Time $\Lambda[ms]$		0.90

was determined from the inverse of the fitted differential worth curve of the control rod, which depends on the temperature and axial control rod positions and has the unit of length per reactivity. For this purpose, a surrogate model was used to predict the value of k_p given these parameters and used directly into Eq. (11) to determine the new axial position of the control rods. Also, some control filters were utilized along with the proportional controller to ensure the predicted control rod axial position is within the physical range of motion of the control rods and to limit their speed. Once the control rod position is determined, it is fed to the power prediction model to calculate the power and check if the new predicted position can reproduce the demanded power signal.

The control rod predictive transient model couples the several components and models to obtain the reactor axial rod positions and total power during the transient experiments along with fuel average temperature as listed below:

- An inverse kinetics model that converts the demand power signal into a reactivity demand signal given the kinetics parameters and time step size.
- A surrogate model that performs polynomial regression of tabulated data based on Serpent calculations to predict the differential rod worth coefficients (k_p) for given axial control rod positions and fuel average temperature.
- A proportional controller that determines the equivalent reactivity of the control rod axial position movement to the calculated demand reactivity signal.
- A surrogate model that performs polynomial regression of precalculated steady state eigenvalue data set using the Serpent code to predict the reactivity in-

troduced in the system given the core average temperature and the predicted axial position of the control rods.

- An adiabatic thermal feedback model that calculates the reactor's average temperature given the heat deposited in the system at each time point.
- A point kinetics model that calculates total power and the delayed neutron precursor concentrations given the predicted reactivity introduced into the system at each time point.

This predictive model relies on a given power signal to derive an equivalent reactivity signal that is required to predict the axial control rod position during a transient. This model has significant value in helping and supporting the design and optimization a new experiments that are going to be irradiated in the TREAT facility. A schematic diagram of the calculation workflow and exchanged parameters of the coupled models are shown in Figure 12.

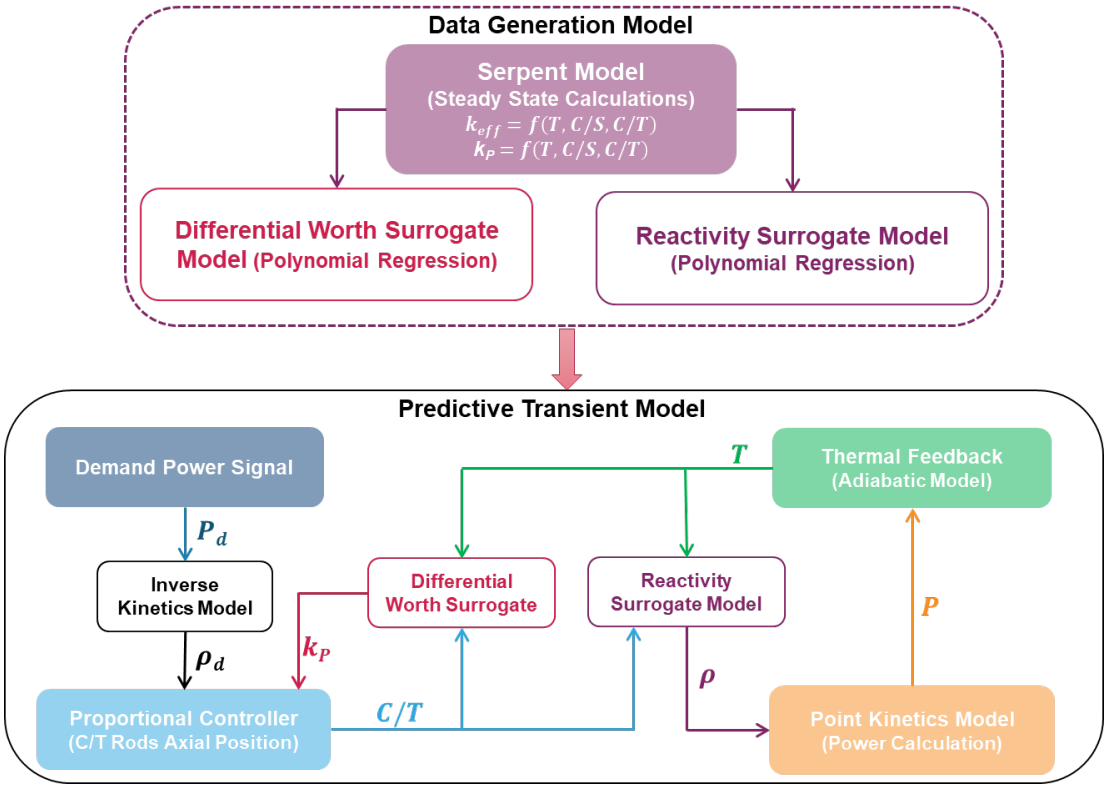

Figure 12: Control rod axial position predictive transient model calculation workflow.

5. Validation Test Results

This section provides validation test results of the predictive transient models against a subset of the Sirius experiments performed at the TREAT facility. The developed models provide a full predictive multiphysics evaluation of the tests to be performed. These models can predict the desired control rod movement to achieve the desired reactor power and energy deposition. In this paper, only the predicted control rod axial position and reactor total power are presented and compared to the measured values for Sirius-1, 2c, and 3. However, the prediction of specimen deposited power and temperature of the Sirius-3 experiment are presented in Ref. [32], and the Sirius-2c results will be presented in future work.

The next two subsections present validation test results of the power predictive model and the predictive model control rod axial position for different tests of the Sirius experiments. However, the differences and specifications are not discussed in this work, and only the reactor power and control rod position are utilized to validate the developed transient model. These tests have a negligible impact on the reactor's total reactivity and power evolution.

5.1. Power Prediction

The forward model is validated using experimental data from the Sirius-1 and Sirius-3 transient tests. These transient experiments were run for about 40 to 80 s, in which the control rods are moved to introduce a positive reactivity to increase the power from a cold state to the megawatt range within a short time. This will lead to a significant increase in the temperature of the fuel sample being irradiated. The length and shape of the power are determined by the total amount of energy that needs to be deposited in the fuel specimen to achieve the desired temperature. The following subsections present the validation test results of the Sirius-1 half, full, and peak power tests, and Sirius-3 full power test.

5.1.1. Sirius-1 Tests

The Sirius-1 experiment was performed at three different power levels: half power (HP), full power (FP), and peak power (PP), as called by the experimenters. The measured control rod axial position of the C/T rods and measured power for all the experiments are shown in Figure 13. Also, Table 2 provides the initial positions of all control rod sets at each power level which is needed for the reactivity surrogate model to accurately predict the total reactivity introduced into the system.

Each transient test can be divided into three regions: prompt reactivity insertion or first peak region (first 10 s of the transient), peak power region (middle of the transient where the peak power occurs), and feedback-controlled region (region after the power peak). The first region of the transient is influenced by initial reactor power, temperature, kinetics parameters, and precise control rod axial positions. The second region is driven by the reactivity worth of the C/T movement (i.e., the reactivity insertion rate) and mild feedback effects. The last region of the transient is driven by thermal feedback of the system resulting from the increased temperature, where the power stabilizes at a certain level and remains at the same level until the end of the transient. In this region, a stronger feedback effect is introduced due to increased fuel temperature, and it is compensated by withdrawing the C/T rods at a level that compensates for the negative reactivity to maintain a constant power level.

Figures 14, 15, and 16 show comparisons of the measured and calculated reactor power using the predictive transient model of the three Sirius-1 experiments for half, full, and peak power tests, respectively, along with calculated core average temperature and measured axial C/T rods position. For all tests, the calculated power is in very good agreement with measured values for all of the transient regions. A small discrepancy was noticed in all three tests after the first peak region, which can be related to (1) poor measured initial power resulting from a very low neutron signal, (2) uncertainty of the exact control rod position as it moves faster in that region, and (3) the uncertainty of the kinetics parameters as they have significant impact on that region of the transient.

For the peak power experiment, a non-negligible deviation of the calculated power from the measured values at the feedback region, which is related to the simplified thermal feedback model, and experimental values of the heat capacity used in the model. The approximations inherent to these models lead to more pronounced differences at higher temperatures. However, the overall performance of the predictive power transient model shows reasonable results for all of the Sirius-1 power tests. The calculated core average temperature of the Sirius-1 tests increases from its initial value of 300 K to 370 K, 520 K, and 540 K for the half, full, and peak tests, respectively.

5.1.2. Sirius-3 Test

To add more confidence to the developed predictive power model, more experiments are analyzed for further testing and validation of the model with the most recent available transient experimental data of the TREAT facility. The Sirius-3 full power

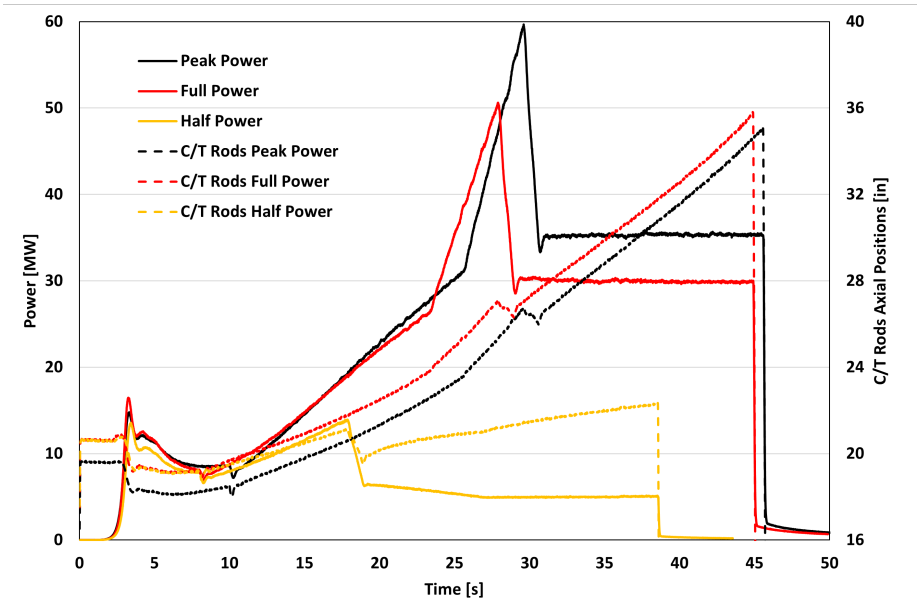

Figure 13: Measured power and C/T rods axial positions during Sirius-1 Transient Experiments.

Table 2: Sirius-1 control rods initial axial positions.

Experiment	Rod No.	Control Rod Position[in]		
		C/C	C/S	C/T
Half Power	1	58.50	49.20	17.53
	2	59.00	49.40	17.63
	3	58.50	49.20	17.59
	4	58.60	49.00	17.52
	Avg.	58.65	49.20	17.57
Full Power	1	58.40	48.10	17.42
	2	59.00	49.50	17.54
	3	58.50	49.50	17.60
	4	58.70	49.50	17.52
	Avg.	58.65	49.15	17.52
Peak Power	1	58.40	54.80	16.42
	2	59.00	54.70	16.51
	3	58.50	54.90	16.60
	4	58.70	54.80	16.57
	Avg.	58.65	54.80	16.53

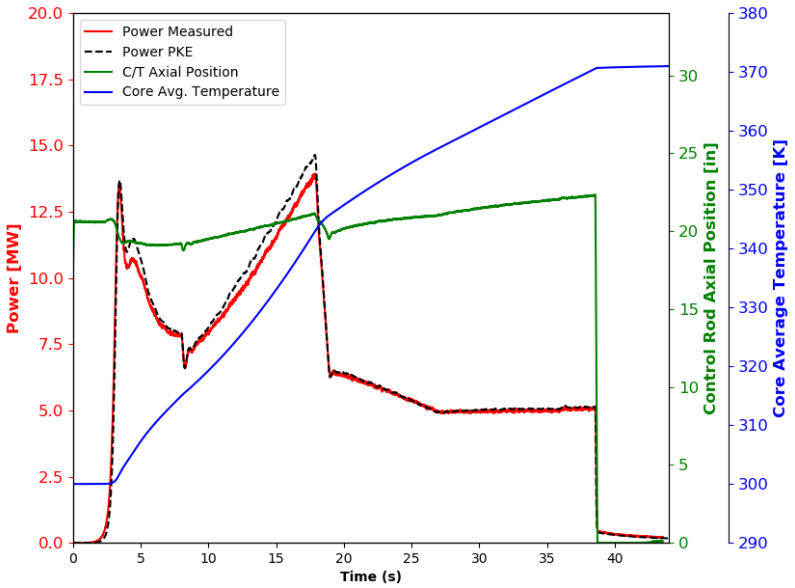

Figure 14: Comparison of the predicted and measured powers for Sirius-1 half power test.

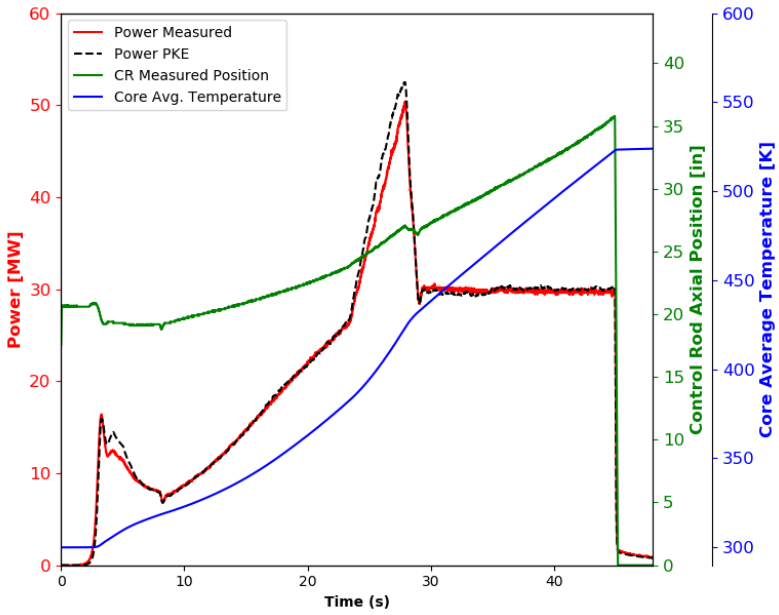

Figure 15: Comparison of the predicted and measured powers for Sirius-1 full power test.

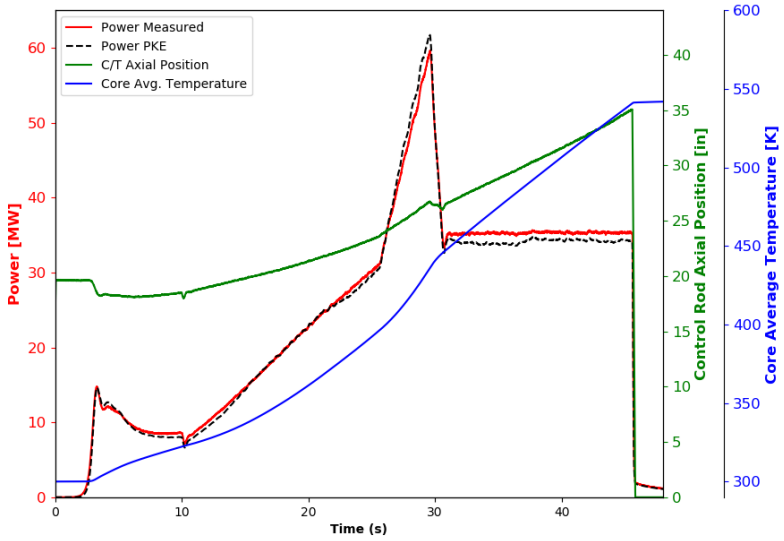

Figure 16: Comparison of the predicted and measured powers for Sirius-1 peak power test.

test is simulated, and the predicted power evolution during the test is compared to the measured values in Figure 17. This test is different than the previous test in terms of initial control rod position, peak power, power evolution, power shape during the transient, and the length of each transient region, specifically the long thermal feedback region.

Similar to the previous tests, the predicted power is in very good agreement with measured values for the whole experiment duration except for the time between 5-10 s (after the first peak), which shows that the power is slightly overestimated and then underestimated. This might be explained by large uncertainty in the initial power and control rod position at that point of the transient. However, for the remaining period of the transient, the calculated power matches the measured value at the peak region and thermal feedback region.

5.1.3. Model Performance

In order to assess the performance of the power prediction model, the predicted power is compared to the measured values considering peak power relative difference, the average relative difference or the root mean square value (RMS), and the integral of the difference for the whole transient period along with peak power value and time to achieve that peak. For the Sirius-1 tests, the peak error is between 3.0% to 5.0% and the integral error is about 5.0% for different peak power values and peak

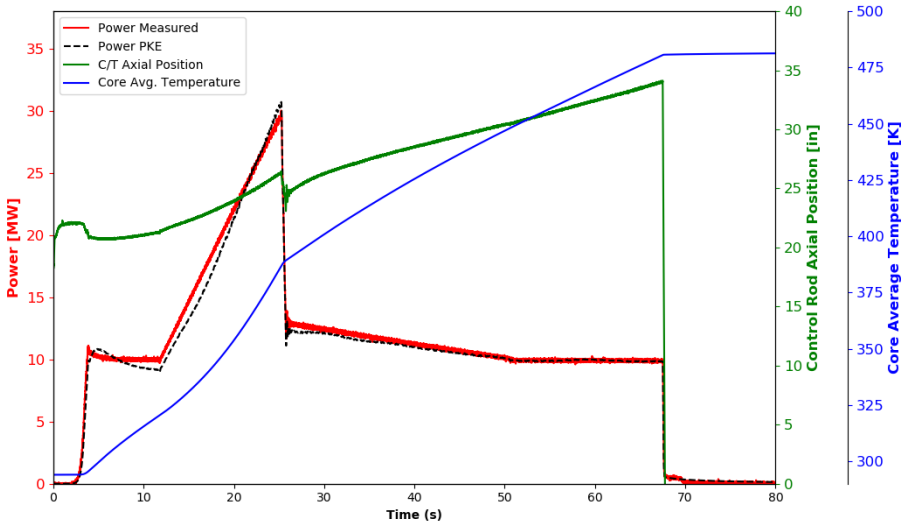

Figure 17: Comparison of predicted and measured power for Sirius-3 full power test.

time. Similar performance is also observed for Sirius-3 full power test where the peak error is about 3.0% and integral error of 3.6%. Table 3 provides the peak power information and power relative errors compared to the measured power for Sirius 1 and 3 tests.

Table 3: Performance of power predictive model for predicting the reactor power.

Sirius Test		Peak		Power Relative Error (%)		
Number	Name	Power [MW]	Time [s]	Peak	Integral	RMS
1	Half Power	14.64	17.85	4.98	5.60	14.80
1	Full Power	52.53	28.05	3.57	6.05	13.86
1	Peak Power	61.73	29.60	3.33	5.72	13.69
3	Full Power	30.70	25.24	2.82	3.57	5.64

5.2. Control Rods Axial Position Prediction

Knowing the movement and the axial position of the control rod that will result in a certain power shape is very valuable to support the design of new experiments in achieving the desired outcome of the sample temperature. The predictive control rod axial position was developed to fulfill this purpose, and it relies on the demand power

signal to predict the axial control rod movement that will result in a similar power evolution. The predictive control rod axial position was tested and validated using the experimental data of the Sirius-1 full power test and Sirius-2c calibration, half, and full power tests. The Sirius-2c tests are the most recently available experimental data of the Sirius experiments conducted at the TREAT facility.

5.2.1. Sirius-1 Test

The Sirius-1 full power test is used to validate the predictive control rod axial position and compare its results to the predictive power model. The measured power signal was used as a demand power to predict the control rod axial position during the Sirius-1 full power test. Figure 18 shows the measured power (solid red line) and control rod axial positions of the C/T rods (solid yellow line), along with calculated power with power predictive model (dashed black line) given the measured axial rod position, and the calculated power with control rod predictive model (doted purple line) and predicted axial positions of the C/T rods (doted green line) given the measured demand power signal (measured power).

The results of the power predictive model show noticeable differences in certain regions, after the first peak region (about 5.0 s to 8.0 s) and the second peak (about 25.0 s to 30.0 s), where the control rods are promptly withdrawn or inserted to the core region which will introduce a large uncertainty and delay in the measured axial rod position. But the predictive control rod axial position model was able to mimic the demand or measured power signal, especially the first and second peaks regions, and provide a prediction of the axial control rod positions. However, the measured power signal has huge fluctuations specifically at low power and steady-state or asymptotic power regions due to large uncertainties of the detector readings.

5.2.2. Sirius-2c Tests

A new set of tests was recently conducted at the TREAT test facility to test a different NTP fuel type known as Sirius-2c. For these tests, a demanded power signal was utilized to predict the axial control rod position and total reactor power for calibration, half, and full power tests. Figures 19, 20, and 21 show the prediction for the C/T control rod motion during the transient compared with the anticipated control rod motion for calibration, half, and full power tests, respectively. In addition, the reactor demand and predicted power values are plotted along with the predicted reactor average temperatures. The predictions of the control rod motions are very similar to the anticipated motion, especially for the half-power and full power experiments. Also, these predicted control rod motions resulted in predicted reactor total

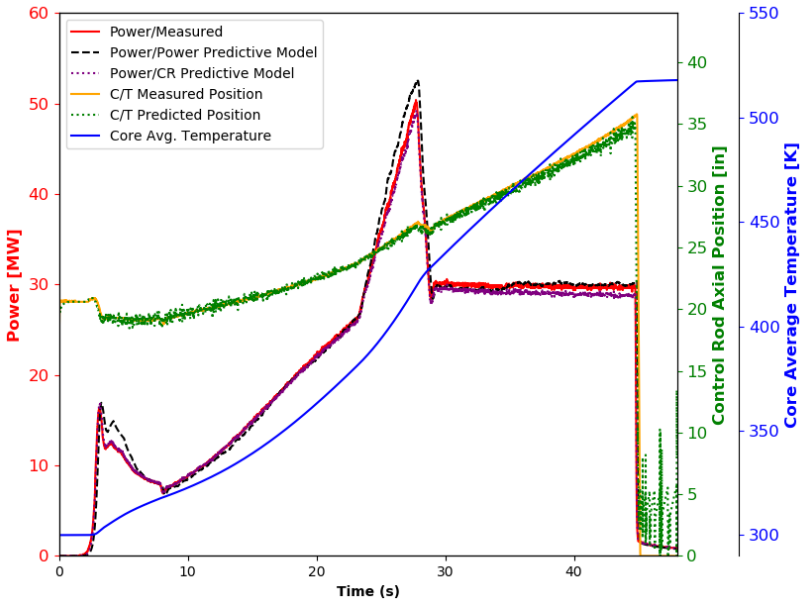

Figure 18: Comparison of predicted and measured power and control rod axial position for Sirius-1 full power test.

power that is in good agreement with the demanded power.

The actual control rod motions were not available at the time of performing the calculations and the model was used to predict the control rod's motion before experiment or blind prediction. The predicted values will be compared to the measured values once it is available for testing its accuracy. The predicted control rod motion exhibits a noisy response at the end of the calibration power test. This is caused by the noisy reactor power signal at a low level, which occurs when the speed of the control rod motion changes significantly within a short period.

5.2.3. Model Performance

The performance of the control rod predictive model is assessed for Sirius-1 full power test and Sirius-2c tests compared to the measured or demand power. Table 4 provides the peak power information and power relative errors and Table 5 provides relative errors of the C/T rods position for Sirius-1 full power and Sirius-2c tests. For Sirius-1 full power test the peak error is about 2.82% and integral error is about 2.76% which is reduced compared to the power prediction model where the peak error is about 3.57% and integral error is about 6.05%. The error in the predicted control rod position at the peak location is 0.70% and integral error is 0.88%. For

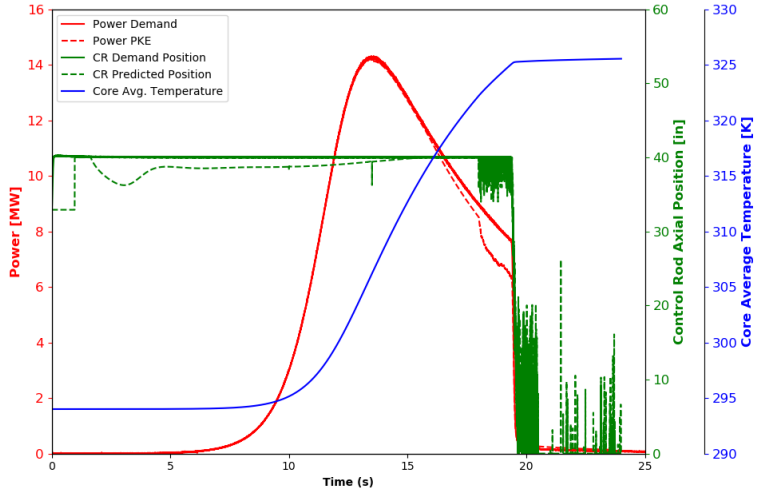

Figure 19: Comparison of predicted and measured power and control rod axial position for Sirius-2c calibration power test.

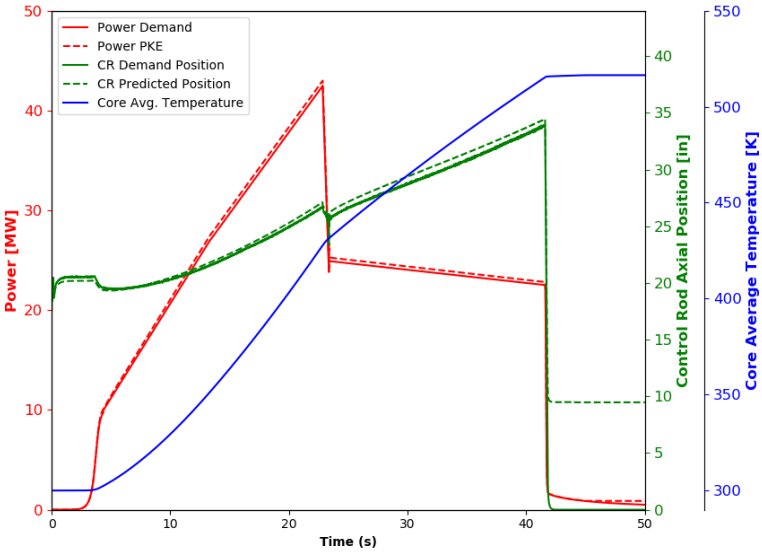

Figure 20: Comparison of predicted and measured power and control rod axial position for Sirius-2c half power test.

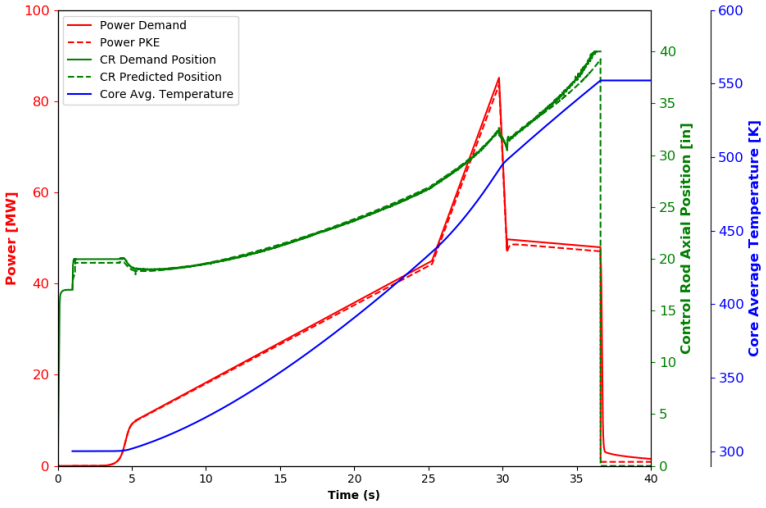

Figure 21: Comparison of predicted and measured power and control rod axial position for Sirius-2c full power test.

Sirius-2c tests, the model performs well with peak power and integral power errors of less that 2.0%. For the Sirius-2c calibration test the RMS is little high which is affected by the last part of the transient due to noisy power signal in that region. Similarl, the predicted control rod position at the peak location and integral error is less than 2.0%.

Table 4: Performance of control rod model for predicting the reactor power.

Sirius Test		Peak			Power Relative Error (%)		
Number	Name	Power [MW]	Time [s]	C/T [in]	Peak	Integral	RMS
1	Full Power	49.27	27.75	26.52	2.82	2.76	8.16
2c	Cal Power	14.24	13.34	39.39	1.31	27.37	234.21
2c	Half Power	43.00	22.84	26.88	1.22	1.82	2.42
2c	Full Power	83.59	29.76	32.25	1.83	1.52	1.65

Table 5: Performance of control rod predictive model for predicting C/T rods position.

Sirius Test		C/T Position Relative Error (%)		
Number	Name	Peak	Integral	RMS
1	Full Power	0.70	0.88	1.18
2c	Cal Power	1.46	2.63	3.49
2c	Half Power	0.96	1.54	1.70
2c	Full Power	0.93	0.76	1.17

6. Summary

Predictive transient models were developed for the TREAT facility to provide the reactor total power and the required control rod axial movement that will produce the demanded power. The models have several components that incorporate a point kinetics model, an adiabatic feedback model, reactivity and control rod worth surrogate models, a proportional controller, an inverse kinetics model, and leverage a high fidelity Serpent model of the TREAT facility to precalculate eigenvalues at different state points. These models are utilized for experiments modeling and simulation to support transient analysis of the NASA-sponsored Sirius experiments at the TREAT facility.

The Serpent model of TREAT was first validated against measured control rod worth and used to understand the behavior of the important reactor parameters such as integral rod worth, feedback coefficient, leakage, and spectral changes of the core at different reactor states. Then, the power prediction model was developed by solving the forward problem given the control rod's axial position during the transient. The model was validated against experimental data of the Sirius-1 half, full, and peak power tests, and the Sirius-3 full power test. By providing the measured control rod axial position during the experiment knowing the fuel average temperature to calculate the total reactivity introduced into the system with a surrogate reactivity model based on the MOOSE stochastic tools module and Griffin neutronics code. The validation test results showed very good agreement with measured power at different power levels and considering various control rod movements.

The ultimate goal of developing these transient models is to predict the motion of the control rod during a transient prior to performing the experiment. To fulfill this goal, a more sophisticated model was developed to predict the axial position and movement of the control rod of the TREAT facility to produce the desired power output. The model solves an inverse problem that combines different models

to predict the position of the control rod during the transient. The model was validated against the Sirius-1 full power test. Also, the model was used to perform blind prediction of the Sirius-2c calibration, half, and full power tests providing a demanded power signal that was utilized along with reactivity surrogate model, the power prediction model, and a proportional controller to predict the control rod axial position. The results were in very good agreement with the measured control rod position and power of the Sirius-1 full power test. For the Sirius-2c tests, the model was able to reproduce a demanded power signal for all tests and predict the axial control rod movement.

This model will help the reactor engineering team of the TREAT facility in preparing and predicting the power and temperature of the experiment. Also, the model helps in reducing the computational time significantly compared to a dynamic 3-D model without losing accuracy level and allows to perform uncertainty quantification for the whole transient. The major drawback of the current model is that it cannot currently separate the reactivity components. Instead, the total inserted reactivity is calculated. Also, to enhance the accuracy of the model, more data points need to be collected and used in the surrogate model to obtain a better predictive reactivity model. Furthermore, a more sophisticated thermal feedback model needs to be considered to account for temperature distribution within the core. Future work will be focused on coupling the current predictive model with the thermal mechanics model to be able to predict the temperature of the tested fuel samples and applying the same approach to different reactor types.

Acknowledgement

This manuscript has been authored by Battelle Energy Alliance, LLC/Idaho National Laboratory for NASA's Space Nuclear Propulsion (SNP) project in the Space Technology Mission Directorate (STMD). The work was performed under Contract No. DE-AC07-05ID14517 with the U.S. Department of Energy. The U.S. Government retains and the publisher, by accepting the article for publication, acknowledges that the U.S. Government retains a nonexclusive, paid-up, irrevocable, worldwide license to publish or reproduce the published form of this manuscript or allow others to do so, for the U.S. Government purposes.

This research made use of the resources of the High Performance Computing Center at Idaho National Laboratory, which is supported by the Office of Nuclear Energy of the U.S. Department of Energy and the Nuclear Science User Facilities.

References

[1] A. Levinsky, V. Valtavirta, F. Adams, V. Anghel, Modeling of the spert transients using serpent 2 with time-dependent capabilities, Annals of Nuclear Energy, 125, 80–98 (2019).

[2] D. Ferraro, et al., Serpent and tripoli-4 transient calculations comparisons for several reactivity insertion scenarios in a 3d minicore benchmark, Proceedings of Mathematics and Computational Methods Applied to Nuclear Science and Engineering, 2019.

[3] B. Sjenitzer, J. Hoogenboom, General purpose dynamic monte carlo with continuous energy for transient analysis, Proceedings of PHYSOR, 2012.

[4] C. Takasugi, N. Martin, V. Laboure, , J. Ortensi, K. Ivanov, M. Avramova, Preservation of kinetics parameters generated by monte carlo calculations in two-step deterministic calculations, EPJ Nuclear Sci. Technol (2023).

[5] D. Levack, J. Horton, C. Joyner, T. Kokan, F. Widman, B. Guzek, Mars ntp architecture elements using the lunar orbital platform-gateway, Proceedings of the AIAA SPACE and Astronautics Forum and Exposition, 2018.

[6] M. DeHart, S. Schunert, V. Labouré, Nuclear Thermal Propulsion. In Nuclear Reactors, Chapter 7, JPope, C.L., Ed., IntechOpen: London, UK, 2022.

[7] T. Jing, S. Schunert, V. Labouré, M. DeHart, C. Lin, J. Ortensi, Multiphysics simulation of the nasa sirius-cal fuel experiment in the transient test reactor using griffin, Energies, 15, 6181 (2022).

[8] R. O'Brien, D. Burns, N. Woolstenhulme, D. Dempsey, C. Hill, C. Hale, The sirius-1 nuclear thermal propulsion fuels transient test series in the idaho national laboratory treat reactor, Proceedings of the Nuclear and Emerging Technologies for Space (NETS), 2019.

[9] M. DeHart, F. Gleicher, S. Schunert, I. Trivedi, Thermal modeling and analysis of the sirius-2 experiment, Transactions of the American Nuclear Society Winter Conference, 2022.

[10] D. Gaston, C. Newman, G. Hansen, D. Lebrun-Grandié, Moose: a parallel computational framework for coupled systems of nonlinear equations, Nuclear Engineering and Design (2009).

[11] R. Williamson, J. Hales, S. Novascone, M. Tonks, D. Gaston, C. Permann, D. Andrs, R. Martineau, Multidimensional multiphysics simulation of nuclear fuel behavior, Journal of Nuclear Materials (2012).

[12] J. Ortensi, Y. Wang, V. Laboure, Z. Prince, C. Lee, Y. Jung, H. Park, E. Shemon, Griffin software development plan, Tech. Rep. INL/EXT-21-63185, Idaho National Laboratory (2019).

[13] A. Slaughter, Z. Prince, P. German, I. Halvic, W. Jiang, B. Spencer, S. Dhulipala, D. Gaston, Moose stochastic tools: A module for performing parallel, memory-efficient in situ stochastic simulations, SoftwareX (2022).

[14] M. Jaradat, W. Yang, An adaptive time-stepping control algorithm for molten salt reactor transient analyses, Annals of Nuclear Energy (2023).

[15] M. Kreher, K. Smith, B. Forget, Direct comparison of high-order/low-order transient methods on the 2d-lra benchmark problem, Nuclear Science and Engineering, 196, 409-432 (2022).

[16] K. Ott, R. Neuhold, Introductory Nuclear Reactor Dynamics, American Nuclear Society, La Grange Park, Illinois, 1985.

[17] E. Parma, M. Vernon, S. Wright, C. Peters, V. Tikare, P. Pickard, J. Kelly, Global nuclear energy partnership fuels transient testing at the sandia national laboratories nuclear facilities: Planning and facility infrastructure options, Tech. Rep. SAND2007-7308, Sandia National Laboratory (2007).

[18] L. Ramseth, Bringing a nuclear test reactor back to life at inl, idaho falls, Tech. Rep. October, Idaho Falls Post Register, Idaho National Laboratory (2014).

[19] D. MacFarlane, G. Freund, J. Boland, Hazards summary report on the transient reactor test facility (treat), Tech. Rep. ANL-5923, Argonne National Laboratory (1958).

[20] C. Bean, F. McCuaig, J. Handwerk, The fabrication of the fuel elements for the transient test reactor, Tech. Rep. ANL-FGF-162, Argonne National Laboratory (1959).

[21] J. Bess, M. DeHart, Baseline assessment of treat for modeling and analysis needs, Tech. Rep. INL/EXT-15-35372, Idaho National Laboratory (2015).

[22] J. Leppänen, M. Pusa, T. Viitanen, V. Valtavirta, T. Kaltiaisenaho, The serpent monte carlo code: Status, development and applications in 2013, Annals of Nuclear Energy, 82, 142–150 (2013).

[23] J. Ortensi, A. Alberti, Y. Wang, M. DeHart, F. Gleicher, S. Schunert, T. Palmer, Methodologies and requirements for the generation of physics data inputs to mammoth transient simulations in support of the transient reactor test facility, Tech. Rep. INL/EXT-15-36265, Idaho National Laboratory (2015).

[24] J. Ortensi, B. Baker, S. Schunert, Y. Wang, F. Gleicher, M. DeHart, Updates to the generation of physics data inputs for mammoth simulations of the transient reactor test facility - fy2016, Tech. Rep. INL/EXT-16-39120, Idaho National Laboratory (2016).

[25] B. Baker, J. Ortensi, M. DeHart, Y. Wang, S. Schunert, F. Gleicher, Analysis methods and validation activities for mammoth using m8 calibration series data, Tech. Rep. INL/EXT-16-40023, Idaho National Laboratory (2016).

[26] B. Baker, J. Ortensi, M. DeHart, Fy 2017 modeling of the m8 calibration series using mammoth, Tech. Rep. INL/EXT-17-42415, Idaho National Laboratory (2018).

[27] N. Todreas, M. Kazimi, Nuclear Systems, Vol. I: Thermal Hydraulic Fundamentals, CRC Press, 2012.

[28] M. Jaradat, S. Schunert, F. Gleicher, V. Labouré, M. DeHart, A predictive transient model of the treat-sirius experiments, Nuclear and Emerging Technologies for Space (NETS), 2023.

[29] J. J. Duderstadt, L. J. Hamilton, Nuclear Reactor Analysis, John Wiley & Sons, Inc.

[30] D. Okrent, C. Dickerman, J. Gasidlo, D. O'Shea, D. Schoeberl, The reactor kinetics of the transient reactor test facility (treat), Tech. Rep. ANL-6174, Argonne National Laboratory (1960).

[31] V. Laboure, S. Schunert, S. T. Z. Prince, J. Ortensi, C. Lin, L. Charlot, M. DeHart, Automated control for nuclear thermal propulsion start-up using moose-based applications, Progress in Nuclear Energy (2023).

[32] F. Gleicher, M. Jaradat, S. Schunert, M. DeHart, Thermal analysis of the sirius3 nuclear propulsion fuel calibration experiment, Nuclear and Emerging Technologies for Space (NETS), 2023.